RECENT RESULTS IN DEEP INELASTIC SCATTERING AT HERA*

K.C. HOEGER
member of the H1 Collaboration
Department of Physics and Astronomy
Manchester University
Manchester M13 9PL, England

(Received October 11, 1994)

Recent experimental results in deep inelastic *ep* scattering from the H1 and ZEUS experiment at HERA are presented. These include the latest measurements on the structure function F_2, a measurement of $\alpha_S(M_Z^2)$ with jets, charged particle spectra in the Breit frame and studies with events exhibiting large rapidity gaps.

PACS numbers: 13.60. Hb

1. Introduction

In summer 1992 the new HERA accelerator became operational colliding proton and electron beams with beam energies of $E_p = 820$ GeV and $E_e = 26.7$ GeV. Such collisions allow to study *ep* interactions in two well separated domains of Q^2, namely deep inelastic scattering (DIS) which can be detected for $Q^2 > 5$ GeV^2 and the quasi-real photon-proton interactions at very small Q^2 ($Q^2 \approx 10^{-2}$). This presentation will concentrate on experimental results from the domain of deep inelastic scattering. Results in the field of photoproduction at HERA are shown in another presentation at this school.

As the first machine of its kind HERA has allowed to extend the accessible ranges both for Bjorken x and for Q^2 by two orders of magnitude. The two experiments at the machine, H1 and ZEUS can detect events from deep inelastic *ep* scattering down to $x \approx 1 \cdot 10^{-4}$ and up to $Q^2 \approx 6 \cdot 10^4$ GeV^2.

---

* Presented at the XXXIV Cracow School of Theoretical Physics, Zakopane, Poland, June 1–10, 1994.

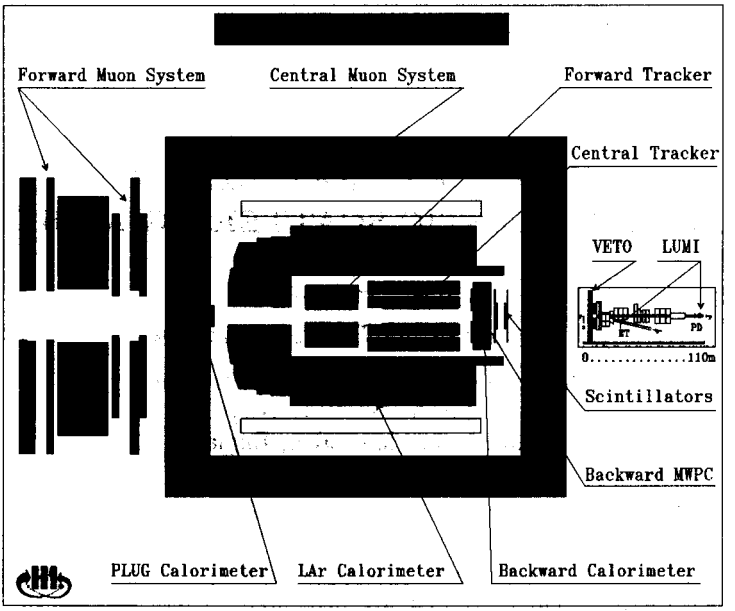

Fig. 1. Schematic view of the H1 detector at HERA. The cut is along the beam axis. Protons enter from the right and electrons from the left.

Apart from the considerable extension of the kinematically observable domain both experiments offer the possibility to perform detailed studies of the hadronic final states with almost complete angular coverage.

The experimental results from both experiments which are presented here are a selection from the ongoing analysis of deep inelastic ep scattering data taken in 1993. During the measurement period of that year the H1 experiment recorded events equivalent to an integrated luminosity of $\approx 530\ \mathrm{nb}^{-1}$ which is more then twenty times the statistics gathered in 1992. Similar numbers hold for the ZEUS experiment.

The experimental setup of the detectors is exemplified here with a brief description of the H1 detector. Detailed descriptions of the H1 and ZEUS detectors can be found in [1] and [2]. A schematic transversal view of the H1 detector is given in Fig. 1 where protons enter the detector along the axis from the right and electron enter from the left. At the HERA experiments the z coordinate is chosen to coincide with the proton direction which is also called the forward direction. Therefore angles are usually measured from the proton direction as well, so that the electrons at small Q^2 typically appear in the back of the detector at ϑ around 170 degrees. The asymmetric detector design reflects the largely different beam energies. The innermost region of the detector surrounding the interaction point contains the central

and forward tracking detectors subtending angles from $\vartheta \approx 7$ to $\vartheta \approx 160$ degrees. These detectors are multilayered structures of drift and proportional chambers to give good resolution for charged particle momenta both parallel and transverse to the beam direction. The trackers are surrounded with the liquid argon calorimeter (LAr) with lead and steel absorbers covering angles from ≈ 4 to ≈ 155 degrees. To the rear is the backward electromagnetic calorimeter (BEMC) extending to $\vartheta \approx 176$ degrees, build as a lead-scintillator sandwich calorimeter. The whole experiment is surrounded by the instrumented iron return yoke used as the central muon detector. Downstream and adjacent to the electron and proton beam line respectively are the electron tagger (ET) at $z = -33$m and the photon detector (PD) at $z = -103$m. These are used to monitor the luminosity by detecting coincidences from the QED Compton process at small scattering angles. The electron tagger is also used to mark the so called tagged photoproduction event sample by detecting the scattered electron. Note that these detectors are not drawn to scale in Fig. 1.

The paper is organized as follows: Section 2 deals with the kinematics reconstruction, Section 3 discusses common backgrounds in DIS event samples, Section 4 compiles recent measurements of F_2, Section 5 presents a determination of α_S with jets, Section 6 examines charged track distributions in the Breit current hemispheres and Section 7 gives a short overview of measurements with large rapidity gap events in DIS.

This presentation is to be understood as an overview of some current research activities in deep inelastic scattering at HERA, but not as a detailed description of the results, some of which are still preliminary. Therefore the reader is referred to the primary literature for more detailed accounts of the results presented here.

2. Kinematics reconstruction

Let p, k, k' denote the fourvectors of the incoming proton and electron and the scattered electron respectively. Then DIS kinematics is given by the Lorentz invariants

$$Q^2 := -q^2 := -(k - k')^2 ,$$
$$x = \frac{Q^2}{2pq} , \qquad y = \frac{pq}{pk} ,$$
$$W^2 = \frac{1-x}{x} Q^2 + m_p^2 .$$

Only two of them are independent, *e.g.* we have $xyS = Q^2$ where $S = 4E_eE_p$. Hence two independent measurements are needed to determine the

kinematics. Since at HERA both the scattered electron and the hadronic final states are observable this leads to a number of kinematics reconstruction methods, the more powerful ones being those which combine electron and hadron measurements. Many of these have been studied during the 1990/91 HERA workshop [3].

2.1. Electron method

This is the way the kinematics is usually reconstructed in fixed target deep inelastic scattering experiments. The two measurements are given by the energy and scattering angle of the electron E'_e and ϑ'_e. From this we get:

$$Q^2_{el} = 4E_e E'_e \cos^2 \frac{\vartheta'_e}{2} \Rightarrow \frac{\Delta Q^2_{\mathrm{el}}}{Q^2_{\mathrm{el}}} \approx \frac{\Delta E'_e}{E'_e}$$

$$y_{el} = 1 - \frac{E'_e(1-\cos\vartheta'_e)}{2E_e} \Rightarrow \frac{\Delta y_{\mathrm{el}}}{y_{\mathrm{el}}} \propto \frac{1}{y}.$$

This means that the Q^2 resolution is always well under control while the measurement of y gets very poor at small y implying a poor resolution on x in that domain as well. The relative accuracy on Q^2 is better then $\approx 6\%$ everywhere but the y measurement is restricted to $y \leq 0.1$. Within the domain $y \geq 0.1$ the electron measurement gives the best resolution of all the methods described here.

2.2. Hadron method

The hadrons in the final state can be measured in a large angular domain $(4 < \vartheta < 170)$ degrees but a lot of energy related to the remains from the beam proton is lost at small angles in the beam pipe. Therefore only 3 components of the fourvector of the hadronic final state can be measured. Since the missing energy in the beam pipe is almost exactly aligned along the axis the total $(E - P_z)^{\mathrm{had}}$ receives a negligible contribution from the lost energy and the same is true for the two components of the transverse momentum $\vec{p}_t^{\,\mathrm{had}}$ of the hadronic final state fourvector. Evaluating y with the final state hadrons we get

$$y_{\mathrm{had}} = \frac{1}{2E_e} \sum_{\mathrm{hadrons}\ i} (E_i - p_{zi})$$

and find for the resolution $\Delta y_{\mathrm{had}}/y_{\mathrm{had}} \approx$ const (typically 20 to 30%). This quantity is also known under the name y Jaquet-Blondel [4]. Calorimeter noise limits the reconstruction of this quantity to $y \geq 0.02$ while the full

reconstruction of kinematics with the hadron method is limited to a rather restricted domain at $x \geq 10^{-2}$ [3].

2.3. Mixed method

This method is defined by the combination of Q^2 measurement with the scattered electron and the y measurement with the hadrons. Then x is given by $x_{\mathbf{mix}} = S/(y_{\mathrm{HAD}} Q^2_{\mathrm{EL}})$. This allows to cover large domains with only mild variations of the resolution of the x and Q^2 measurements.

2.4. Double angle method

This method uses two angles to define the kinematics. One angle is the scattering angle of the electron, the other angle is constructed from the hadronic final state. The latter angle is defined through

$$\tan\frac{\vartheta_{\mathbf{had}}}{2} := \frac{\sum_{\mathbf{hadrons}\ i}(E_i - p_{zi})}{|\sum_{\mathbf{hadrons}\ j}\vec{p_{tj}}|}.$$

Then the kinematical variables x and y are derived from:

$$\tan\frac{\vartheta'_e}{2} = \sqrt{\frac{(1-y)E_e}{xyE_p}},$$

$$\tan\frac{\vartheta_{\mathbf{had}}}{2} = \sqrt{\frac{yE_e}{x(1-y)E_p}}.$$

This gives resolutions similar to the mixed method, without the need to know the absolute calibration of the measured electron and hadron energies. Making the hypothesis that the hadronic final state fourvector is the linear superposition of two massless vectors the above hadron angle can be interpreted as follows. Let the first vector represent the remnants from the beam proton aligned along the z axis and the second vector represent the quark scattered out of the proton by the absorption of the virtual photon then the above hadron direction coincides with that of the current quark momentum.

3. Backgrounds to DIS event samples

This section will describe the sources of background in general terms which apply to all samples of DIS events used in the studies presented in the following sections. The actual selections of events differ slightly from

analysis to analysis and between the two experiments and it is left to the reader to extract the relevant details from the literature.

The background to DIS event samples can be classified into two categories. The first being referred to as technical backgrounds. These arise from interactions of beam particles (protons as well as electrons) with the rest gas in the beam pipe, off track protons hitting the materials in and surrounding the beam pipe if they occur within or close before the interaction region, halo muons traveling parallel to the beam line and cosmic muons. These backgrounds are largely reduced by the trigger system and in the off line reconstruction programs. These backgrounds can be estimated by studying events obtained from the noncolliding proton and electron bunches and are found to be negligible.

On the other hand there are physical backgrounds arising from misidentified "photoproduction" events which at HERA have a much larger cross section then deep inelastic scattering. At HERA the term photoproduction is used for interactions initiated by quasi-real photons where the electron has a very small scattering angle ($Q^2 < 4 - 5\text{GeV}^2$) and does not enter the main detector but remains in the beam pipe. Note that while the vast majority of these events is at $Q^2 \approx 10^{-2}$ the tail of the distribution extends up to $Q^2 \approx 4$ GeV^2.

This leads to backgrounds in DIS samples because energetic hadrons in the backward detectors can be mistakenly identified as "electrons". Approximately 10% of the photoproduction events can be verified as such by detecting the electron under small scattering angles in the electron tagger. These events comprise the so called tagged photoproduction sample. This sample can be used to calibrate MC simulations of γp processes and thereby allows to estimate backgrounds from the untagged photoproduction backgrounds.

Also energy momentum conservation is used to suppress photoproduction backgrounds. This again makes use of the quantity $E - p_z$, however now the summation runs over all particles in the main detector including the scattered electron candidate. We find

$$\delta := \sum_{\text{main detector}} E_i - p_{zi} = \begin{cases} 2E_e & \text{in DIS} \\ 2(E_e - E'_e) & \text{in } \gamma p. \end{cases}$$

Placing a cut at $\delta > 30$ GeV the photoproduction backgrounds are significantly reduced. Further reductions can be obtained by requiring tracker hits to be associated with the electron candidate, thus testing for the presence of a related track and by requiring the lateral and/or transverse shower profiles to be consistent with an electron initiated shower. This allows to achieve negligible backgrounds for large electron energies ($E'_e > 14$ GeV) and reduces the backgrounds to below 10% for low Q^2 and $y \leq 0.7$.

4. Recent measurements of F_2 at HERA

In the domain of low to medium Q^2, ($7 < Q^2 < 2000$ GeV^2) considered here, where deep inelastic ep scattering can be formulated in terms of photon exchange and weak interactions are negligible the double differential cross section is expressible in terms of structure functions as follows:

$$\frac{d^2\sigma}{dxdQ^2} = \frac{2\pi\alpha^2}{xQ^4}\{[1+(1-y)^2]F_2(x,Q^2) - y^2F_L(x,Q^2)\}.$$

The structure functions F_2 and F_L are defined by the decomposition of the differential cross section with respect to the polarizations of the mediating vector boson (the photon). This representation makes no reference to the parton model of hadrons.

Within the framework of QCD F_L can be calculated in terms of the parton distributions and is found to be of order $\mathcal{O}(\alpha_S)$.The contributions of F_L to $d^2\sigma/dxdQ^2$ are small for not to large y. Within the accessible

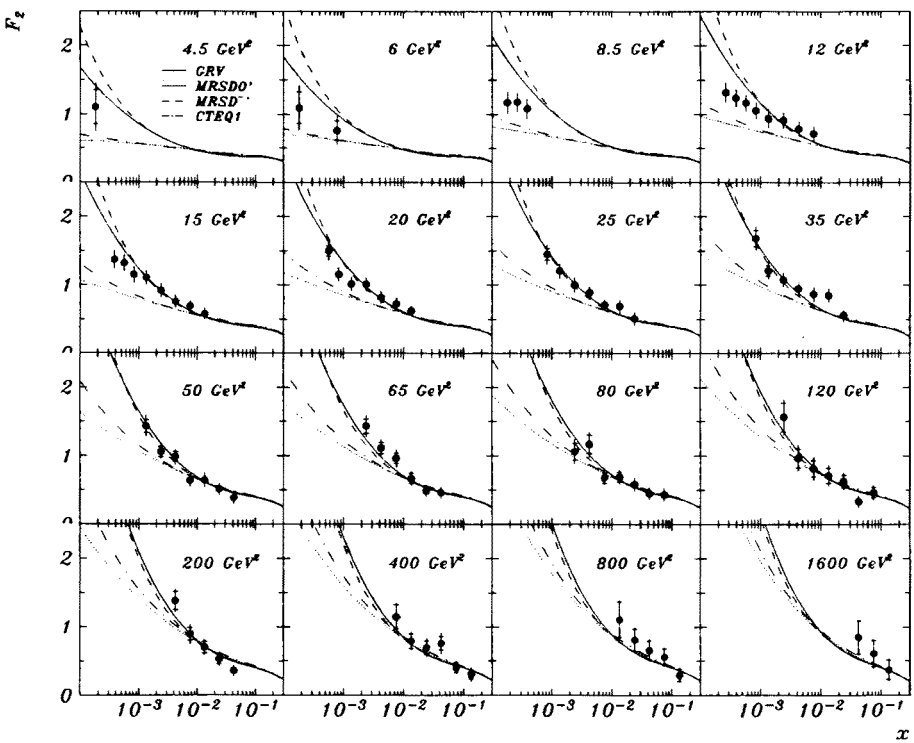

Fig. 2. Preliminary measurement of F_2 as a function of x in various Q^2 bins obtained by the H1 experiment.

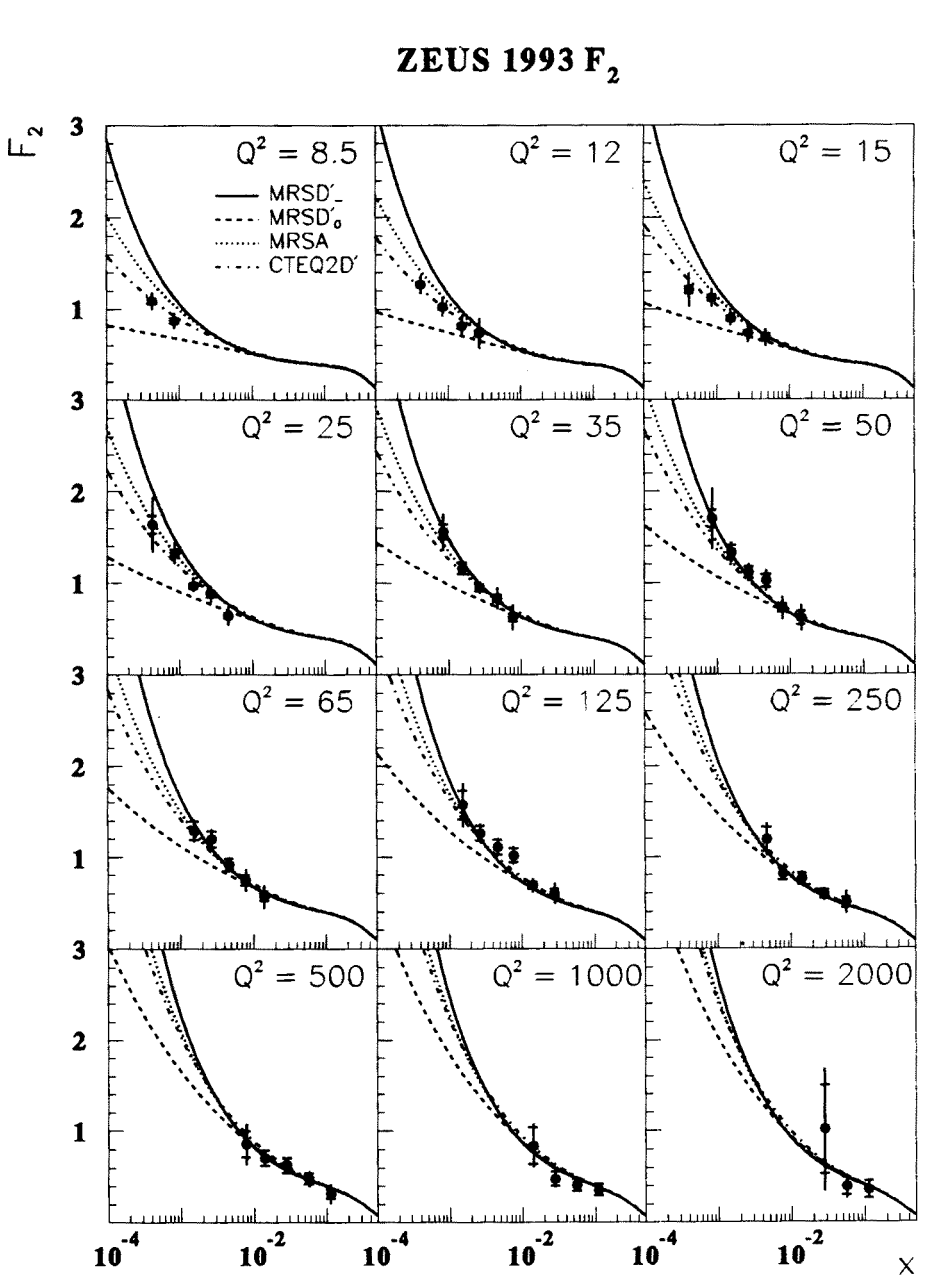

Fig. 3. Preliminary measurement of F_2 as a function of x in various Q^2 bins obtained by the ZEUS experiment.

domain at HERA ($y \leq 0.7$ because of the γp backgrounds) estimates using different parton density parameterizations give relative contributions of up

to 8% at the highest y values. Therefore F_L can be treated as a correction in the derivation of F_2 from $d^2\sigma/dxdQ^2$. This correction appears as a factor R_{QCD} defined through $F_L = F_2\, R/(1+R)$. We then obtain:

$$\frac{d^2\sigma}{dxdQ^2} = \frac{2\pi\alpha^2}{xQ^4}\left[2(1-y) + \frac{y^2}{1+R_{QCD}}\right] F_2(x,Q^2)\,[1+\delta_r(x,Q^2)]\,.$$

Besides the R_{QCD} correction this also contains radiative corrections $\delta_r(x,Q^2)$ which are to be calculated in QED. They account for photon emission and virtual corrections at the lepton vertex. This correction can strongly depend on the method chosen for the determination for the kinematical variables x, y and Q^2. In case of the electron measurement they amount to up to 40% whereas they are fairly small for the mixed method. There exist analytical calculations as well as Monte Carlo programs to compute these corrections (see *e.g.* [5] pp 787 ff).

Since several reconstruction schemes have been used to obtain the F_2 measurement at HERA there is a considerable degree of redundancy. This allows to cross check the systematics involved in the measurement and the calculation of the radiative corrections. Preliminary results from H1 and ZEUS shown in Figs 2, 3 where obtained using the electron method, the double angle method and the mixed method. The inner error bars correspond to the statistical errors which vary between 2% and 20% and the outer error bars represent the full errors including estimated systematical errors with a variation between 5% and 20%. For a detailed discussion of these errors see [6] and [7]. The data cover three orders of magnitude both in x and Q^2 but with the current beam energy settings there is no overlap between the kinematical domains covered at HERA and those at fixed target experiments.

5. α_S measurement with jet rates

In lowest order $\mathcal{O}(\alpha_S^0)$ the hadronic final state in neutral current DIS events can be described as follows: A quark is hit by the virtual photon and scattered out of the proton leading to a hard scattered jet in the final state. In addition to this the leftover from the beam proton forms another jet which is aligned along the beam direction. Such events are called 1+1 jet events in the following where the +1 jet corresponds to the beam jet which is always present. In those processes the momentum fraction x_p of the parton (the quark) entering the hard scattering process can be identified with Bjorken x.

In order $\mathcal{O}(\alpha_S)$ processes, two diagrams contribute. Firstly there is the boson-gluon fusion process which probes the gluon density in the proton

and gives rise to a quark antiquark pair with a large invariant mass in the final state. This process leads to a 2+1 jet configuration of the final state hadrons, where now two hard scattered jets are to be observed. Secondly there is the QCD Compton process where the struck quark radiates a gluon giving rise to large invariant masses between the final state quark and gluon. These events also have the 2+1 jet signature. In both cases the momentum fraction x_p of the incoming parton is much larger then Bjorken x. Neglecting transverse momenta of the initial parton we find:

$$x_p = x\left(1 + \frac{\hat{s}}{Q^2}\right). \tag{1}$$

Here $\hat{s}$ is the invariant mass squared of the final state scattered partons arising from the hard scattering process.

In order to compare to QCD calculations a jet reconstruction scheme has to be specified which determines for each event the number of resolved jets. Here this is done with the modified Jade algorithm [8, 9]. This algorithm uses a pseudo-particle aligned along the beam pipe which is constructed in order to account for the unobserved energy at very forward angles. It reduces the number of particles/jets by iteratively merging the pair with the smallest invariant mass until all remaining pair masses exceed the specified resolution ($m_{ij}^2/W^2 \geq y_{\text{cut}}$). The choice to scale the invariant masses with W^2 is driven by the fact that jets close to the proton remnant may not be resolvable. Therefore the proton remnants can get merged into a jet and the whole hadronic final state invariant mass is seen in the clustering procedure.

The jet rate defined as

$$R_{2+1}(Q^2, y_{\text{cut}}) = \frac{\sigma_{2+1}(Q^2, y_{\text{cut}})}{\sigma(Q^2, y_{\text{cut}})}$$

has been calculated up to order $\mathcal{O}(\alpha_S^2)$ for this jet scheme [10] and is available in form of the PROJET Monte Carlo [11]. Measured jet rates were found to be described by such calculations in the domain $y_{\text{cut}} \geq 0.01$ [12]. In the following the cut is placed at $y_{\text{cut}} = 0.02$. The rates depend both on the parton densities and on α_S. In order to obtain an unambiguous extraction of α_S the uncertainties arising from limited knowledge of the parton densities are minimized by a suitable selection of events. For 2+1 jet events we get from equation (1):

$$x_p \geq y_{\text{cut}} + x(1 - y_{\text{cut}}) \geq y_{\text{cut}}\,.$$

Therefore the 2+1 jet cross section for $y_{\text{cut}} \geq 0.02$ is already probing parton densities at large x_p and we can meet the above requirement by imposing the additional cut $x_p \geq 0.01$ for the 1+1 jet sample only.

The general event selection cuts used to have minimal photoproduction backgrounds, reliable electron measurements and sufficient hadronic phase space for jets are

- an electron candidate fulfilling $160 < \vartheta' < 172.5$ degrees, $30 < Q^2 < 100$ GeV^2 and $E_e > 14$ GeV or
  $10 < \vartheta' < 148$ degrees and $Q^2 > 100$ GeV^2 and $y_{el} < 0.7$
- $W^2 > 5000$ GeV^2

The jet rates measured in H1 have been corrected to the parton level using events from the Monte Carlo program LEPTO [13] passed through a full simulation of the detector and the reconstruction software. Results are displayed in Fig. 4(a) and compared with NLO predictions from PROJET for various values of $\Lambda_{4,\overline{MS}}$. These data points are translated into three measurements of $\alpha_S(Q^2)$ using the coefficients calculated in PROJET and shown in Fig. 4(b). The falling band of curves is obtained by fitting $\Lambda_{4,\overline{MS}}$ in the two loop solution of the renormalization group equation whereas the horizontal band of curves is derived assuming a constant $\alpha_S(Q^2)$. The data prefer a running $\alpha_S(Q^2)$.

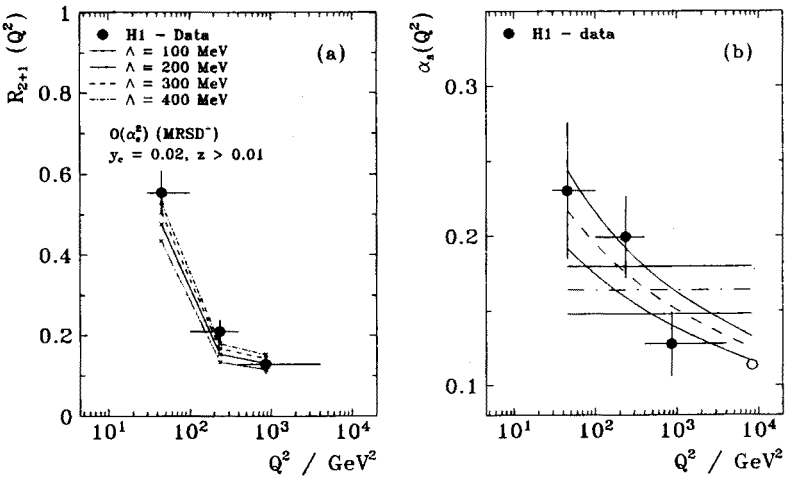

Fig. 4. Preliminary measurement from the H1 Collaboration showing (a) the jet rate as a function of Q^2 with the additional event section cuts requiring $y_{cut} \geq 0.02$ and $x_p \geq 0.01$ and (b) the measurement of $\alpha_S(Q^2)$ derived from the data in (a). The open circle represents the world average at the Z^0 mass.

Combining fits using different parton density parameterizations and extrapolating to $Q^2 = m_Z^2$ gives a preliminary result of $\alpha_S(M_Z^2) = 0.121 \pm 0.010_{\text{stat}} \pm 0.012_{\text{syst}}$ [14] consistent with the current world average [15]. The

systematical error studied so far covers uncertainties in the parton densities, the $y_{\rm cut}$ dependence, variations of the renormalization scale and uncertainties in the calorimetric energy calibration. Uncertainties arising from the correction to the parton level which may be important at small Q^2 are under study and not yet included.

6. Charged particles in the Breit frame

The formation of hadrons in hard scattering processes is currently understood as a three layered process. Firstly there is the primary hard scattering process which results in one or more energetic partons in the hadronic final state besides the leftover from the beam proton. As was shown in the previous section perturbative QCD predictions for these processes can be tested by measurements of jets of final state hadrons. The next layer, namely the process whereby energetic partons evolve into cascades of soft partons is also described by perturbative QCD. Finally colourless hadrons are formed by those partons in the process of hadronization which involves energy scales to small for perturbation theory to be applicable. In this section we shall consider properties of the hadronic final state governed by the parton showering process.

Coherence effects in gluon radiation which is known to dominate in the process of parton showering lead to angular ordering of the emitted gluons. This results in a suppression of the number of soft partons. In order to test predictions obtained in the modified leading log approximation (MLLA) for parton distributions these are linked to the observable distributions of final state hadrons by use of the local parton hadron duality hypothesis [16]. These calculations have been used to interpret measurements of charged particle multiplicities and momentum spectra at LEP and lower energy e^+e^- colliders [17] where it is shown that already the Gaussian approximation to the MLLA gives a good description of the data. The MLLA predicts the $\sqrt{\hat{s}}$ dependence of $\ln 1/x_p$ distributions of inclusive charged particle spectra where $x_p = 2E/\sqrt{\hat{s}}$ is the scaled momentum of charged tracks.

In *ep* deep inelastic scattering the parton shower resulting from the current fragmentation is purely time like as in e^+e^-. However, in *ep* interactions the proton fragmentation region is more complicated, since it contains the space-like initial state parton cascade as well as the remnant from the initial beam proton. In order to compare to the predictions and to e^+e^- data at HERA the *ep* events are studied in the Breit frame. This frame is defined by the two requirements *(i)* the exchanged virtual photon and the incoming proton momenta are antiparallel and *(ii)* the virtual photon is purely space-like. In that frame the proton has the momentum $p^* = Q/2x$ (using $Q = \sqrt{-q^2}$) and lowest order events ($\mathcal{O}(\alpha_S^0)$) are characterized by

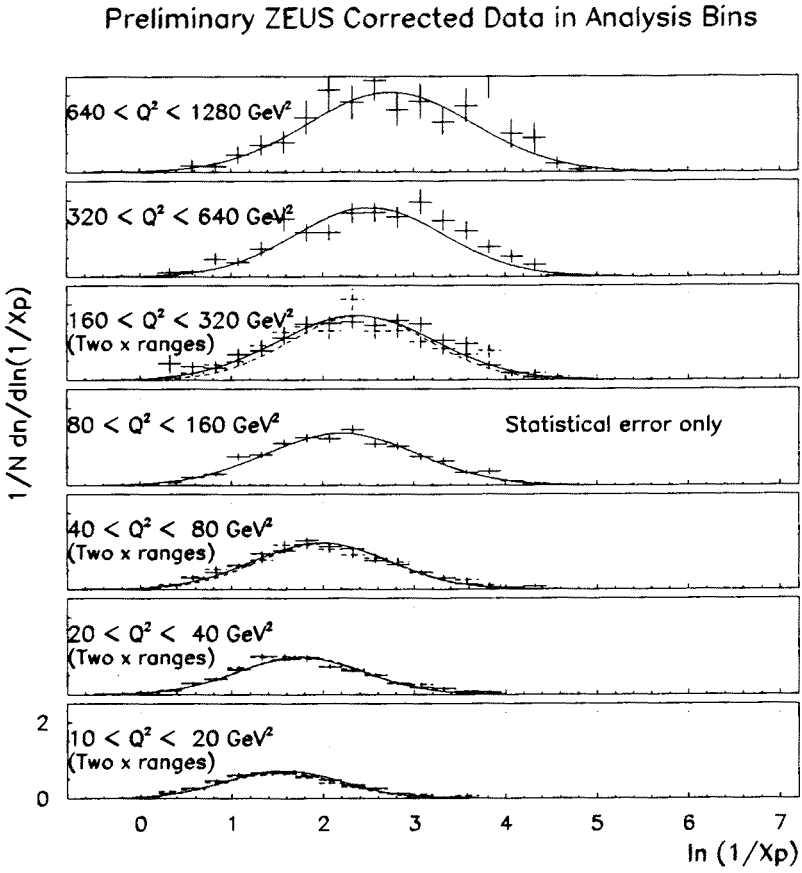

Fig. 5. Preliminary $\ln(1/x_p)$ spectra for charged particles in the Breit frame current hemisphere for various values of Q from ZEUS. Note for some Q bins the distributions for 2 different x have been overlaid. The curves are a guidance to the eye.

an initial quark with momentum $p_z = Q/2$ being backscattered by absorption of the virtual photon ending up with the momentum $p_z = -Q/2$ and no transverse momentum. Then particles with negative p_z constitute the current hemisphere and the rest is denoted as the proton fragmentation hemisphere. Preliminary $\ln(1/x_p)$ distributions obtained by the ZEUS experiment [18] for various Q bins are given in Fig. 5. This clearly shows that the distribution is shifted as a function of Q and that the distribution does not depend on x (and hence W).

In the DIS the energy scale in the current hemisphere is Q. This has to be compared to $\sqrt{\hat{s}}$ setting the scale in e^+e^- collisions. So we have to identify Q^2_{DIS} and $s_{e^+e^-}$. In comparing multiplicities observed in the

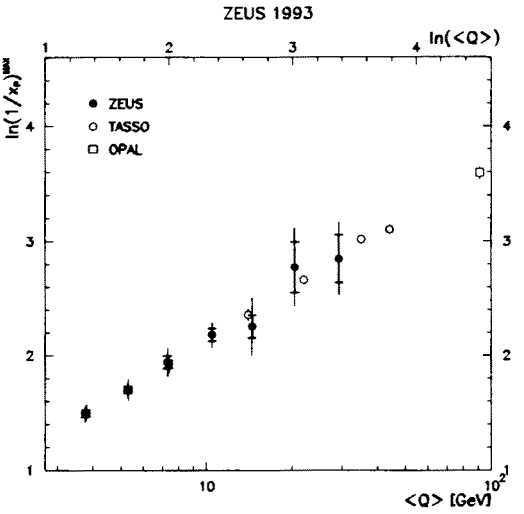

Fig. 6. $\ln(1/x_p^{\max})$ vs Q together with data from e^+e^- data from the TASSO and OPAL experiments identifying $\hat{s}_{e^+e^-}$ and Q_{DIS}. Preliminary result from the ZEUS Collaboration.

Breit current hemisphere in DIS to multiplicities in e^+e^- events the latter have to be divided by a factor two to account for the fact that the Breit current hemisphere corresponds to only half an e^+e^- event. Following these considerations the position of the maxima of the $\ln(1/x_p)$ spectra, their widths and the multiplicities observed in DIS can be compared to those from e^+e^- data and predictions from the MLLA. Preliminary data from the ZEUS Collaboration showing the dependence of $\ln(1/x_p^{\max})$ on Q are shown in conjunction with e^+e^- data in Fig. 6. The same observations have been made by the H1 Collaboration and preliminary results are available in [19]. Fig. 6 shows that within errors DIS data and e^+e^- data follow the same functional dependence and are found to be in accord with the MLLA calculations. In e^+e^- this has been taken as experimental evidence for gluon coherence effects. Since the phase space in the proton fragmentation hemisphere is much larger then that of the current hemisphere and since it contains space-like showers a straightforward comparison to either the current hemisphere or e^+e^- data is not possible.

7. Events with large rapidity gaps in DIS

Observation of events with large rapidity gaps in deep inelastic scattering was first reported by the ZEUS Collaboration at HERA in 1993 [20]. These events are characterized by a large rapidity interval around the proton beam direction devoid of final state hadrons. The corresponding observable

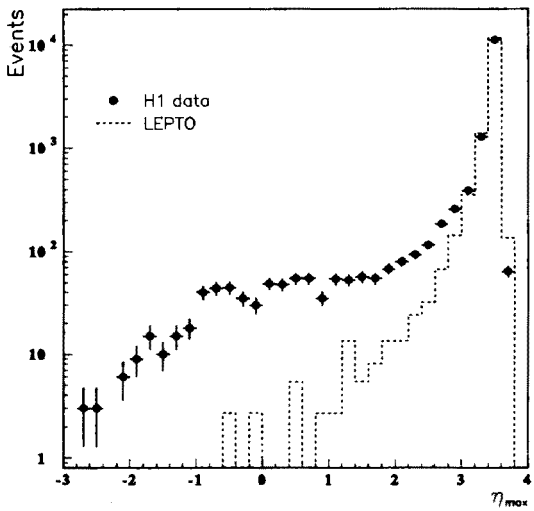

Fig. 7. The η_{max} distribution as obtained by H1. The dashed histogram represents expectations from a standard DIS Monte Carlo program (LEPTO).

η_{max} is defined as the maximum pseudorapidity ($\eta = -\ln\tan\vartheta/2$) of a significant energy deposition ($E > 400$ MeV) in the calorimeters. This establishes the observation of an empty cone covering rapidities from η_{max} up to the geometrical acceptance limit of the detectors. The main calorimeter covers rapidities up to $\eta \approx 3.65$ in H1 and up to $\eta \approx 4.3$ in ZEUS. In Fig. 7 the η_{max} distribution as obtained by the H1 experiment using the standard DIS event selection [21] is shown. The histogram superimposed on the plot shows the expectations for this distribution when deep inelastic scattering off partons in the proton is assumed. The histogram was obtained with the LEPTO Monte Carlo [13]. It is observed that the bulk of the data is at large η_{max} where the first significant energy deposition is close to the geometrical acceptance limit. This part of the distribution is well described by the standard DIS Monte Carlo programs. However, at small η_{max} a comparatively large number of events with large rapidity gaps is observed in the data which cannot be accounted for in the framework of standard DIS event Monte Carlo simulations. In the following the sample of rapidity gap events is defined by the requirement

$$\eta_{max} \leq 1.8\,, \tag{2}$$

in addition to the standard DIS event selection cuts (see Sections 3, 4). Events passing this selection amount to a fraction of approximately 10% of the total DIS event sample. Studying detector components reaching beyond the geometrical acceptance limit of the main calorimeter the H1 Collaboration found evidence for the rapidity gaps in those events to stretch

out beyond $\eta \approx 6$ [21]. A second selective observable is M_X, the invariant mass of all final state hadrons in the main detectors. A plot of M_X vs W shows that the rapidity gap events appear as a distinctive class of events confined to low M_X values for all W (see Fig. 1b in [22]). This again contrasts to standard DIS event Monte Carlos which predict M_X to rise more strongly with W.

Taking this as evidence for a new class of events with large rapidity gaps the question arises whether their kinematical distributions in Bjorken x and Q^2 allow to shed some light on possible production mechanisms. One way to probe this is to study the relative fraction of events passing selection 2 with respect to the full DIS event sample. Forming such ratios one has to keep in mind that the rapidity gap selection (2) introduces a bias against low W events. This is because the current jet in these events may fall into the sensitive rapidity range. Studies with Monte Carlo programs modelling rapidity gap events (see below) show that the acceptance for rapidity gap events levels off to become a flat function of W for $W \geq 140$ GeV. The relative production rates for rapidity gap events using the cut $W \geq 140$ GeV is shown in Fig. 8 as a function of Q^2 for three different x ranges [21]. See also Fig. 2 in [22]. These measurements give no evidence for a strong Q^2 variation of this ratio and show a slight variation of the ratio as a function of x. The absence of a Q^2 variation of these ratios suggest that the production mechanism for the rapidity gap events is of leading twist as is the case for the standard DIS processes.

The large rapidity interval devoid of final state hadrons may be interpreted as a signature of diffractive processes, ie processes in which no colour charge is exchanged in the underlying hard scattering process. One way to model such processes is to assume that a colourless object with the quantum numbers of the vacuum (known under the name pomeron) is exchanged. Furthermore it is assumed that the pomeron behaves like a hadron so that the diffractive events may be modelled as deep inelastic scattering off the partons in the pomeron. The RAPGAP [23] and POMPYT [24] Monte Carlo programs are implementations of such models. They offer a choice between hard ($\beta f(\beta) \propto \beta(1-\beta)$) and soft ($\beta f(\beta) \propto (1-\beta)^5$) parton distributions in the pomeron. The Nikolaev-Zakharow (NZ) model is a non-factorizable variation of this approach [25] where the pomeron interacts as a coherent pair of two gluons with a $q\bar{q}$ pair. A rather different framework to describe such processes is the vector-meson-dominance (VMD) type electroproduction process including diffractive dissociation. These include the possibility for both the vector meson and the incoming proton to dissociate diffractively. See [21] and references therein.

If there is hard scattering off partons in the pomeron then this should lead to subsamples of events with hard jets very much in the same way as

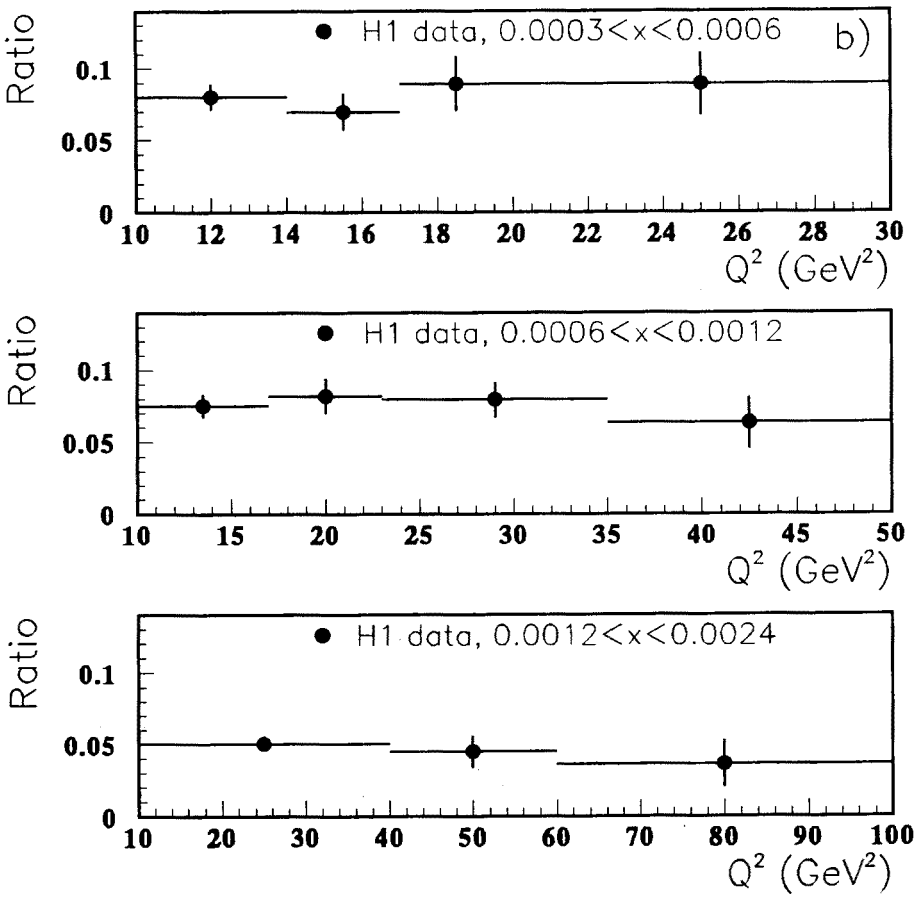

Fig. 8. The ratio of the rapidity gap cross section ($\eta_{\max} < 1.8$) and the standard DIS cross section vs Q^2 for various x bins. Data were selected with the additional cut $W \geq 140$ GeV.

in deep inelastic scattering on hadrons. However, since the pomeron carries only a small fraction of the proton momentum $< x_{\mathrm{Pom}} > \approx 3 \cdot 10^{-3}$, the invariant mass M_X of the virtual photon proton system is much smaller then W^2, thus restricting the available phase space for multi jet events. The ZEUS Collaboration has searched the rapidity gap event sample for jets both in the laboratory and the $\gamma^* p$ center of mass frame. Results using a cone algorithm are published in Fig. 4 of [22]. This study provides evidence for jets and multi jet events with large rapidity gaps. It also shows that larger values for the transverse energies predominantly arise from jets and that the E_T distributions of the jets can be described by the POMPYT and the NZ models.

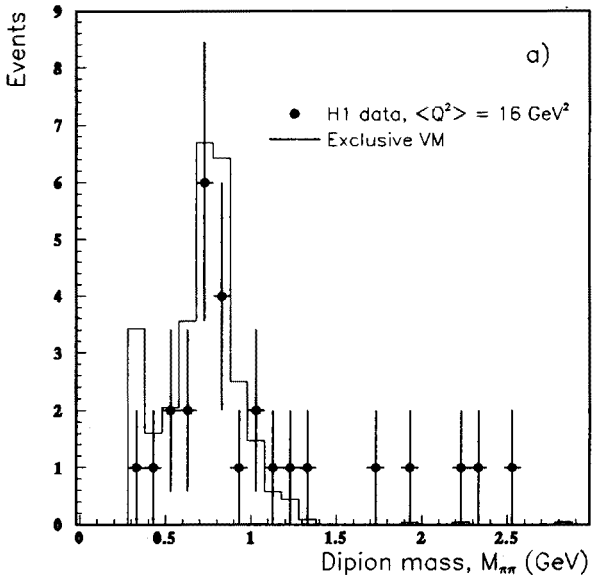

Fig. 9. Invariant mass spectrum from large rapidity gap events with only two tracks of opposite charge. Result from the H1 experiment.

Studying the charged tracks in the sample of rapidity gap events the H1 Collaboration found a seizable fraction of events having only two oppositely charged tracks with no significant energy depositions in the calorimeters beyond what has to be attributed to the tracks [21]. The invariant mass spectra of these two charged tracks using a pion mass hypothesis is given in Fig. 9. This spectrum is found to be consistent with exclusive production of ρ^0, ω and ϕ mesons where ρ^0 production is dominating. Correcting for acceptance losses it is estimated that these exclusive vector meson events account for approximately 10% of the total rapidity gap sample in DIS at HERA. Measurements of electroproduction of exclusive vector mesons at lower energies and slightly smaller Q^2 can be extrapolated to HERA energies. The Rates at HERA are found to be consistent within the large uncertainties of such an extrapolation. These uncertainties are mainly due to the unknown relative magnitude of contributions from longitudinally and transversely polarized photons. See [21] and references therein. Given there is exclusive vector meson production in the rapidity gap sample then it is expected that there are also events arising from diffractive dissociation processes of the vector mesons and/or the beam protons. The above analysis of the H1 Collaborations finds that the η_{max} and M_X distributions can be fully described by a mixture of elastic and inelastic VMD-type processes if the contribution from inelastic processes is allowed to be relatively large.

Summarizing the current measurements using events with large rapidity gaps at HERA they are found to be a distinctive class of events not accountable for in terms of standard DIS events models assuming hard scattering off partons in the proton. Attempts to model these events describe them in terms of diffractive physics. There is evidence for hard scattering off partons in a hypothetical pomeron as well as evidence for VMD-type contributions to this event sample. Various models have been shown to be able to reproduce the shapes of observed distributions but a more quantitative analysis in terms of the involved processes and their relative contributions to the cross sections is not yet possible.

REFERENCES

[1] I. Abt *et al.* (H1 Collaboration), DESY preprint DESY 93-103, 1993.
[2] The ZEUS Detector, Status Report 1993, DESY 1993.
[3] See Proc. Workshop Physics at HERA, DESY, Hamburg, Vol. 1, 1991, p 19 ff.
[4] Jaquet-Blondel, Proc. of the Study for an *ep* Facility, ed U. Amaldi, Hamburg 1979, pp 391-394.
[5] See Proc. Workshop Physics at HERA, DESY, Hamburg, Vol. 2, 1991, p 787 ff.
[6] Measurement of F_2, Contribution of the H1 Collaboration at the 27th International Conference on High Energy Physics, Glasgow, UK, July 1994.
[7] Measurement of F_2, Contribution of the ZEUS Collaboration at the 27th International Conference on High Energy Physics, Glasgow, UK, July 1994.
[8] JADE Collaboration, W. Bartel, *et al., Z. Phys.* **C33**, 23 (1986).
[9] D. Graudenz, N. Magnussen, Proc. Workshop Physics at HERA, DESY, Hamburg, Vol. 1, 1991, p. 261, and contributions therein.
[10] D. Graudenz, *Phys. Lett.* **B256**, 518 (1991); D. Graudenz, *Phys. Rev.* **D49**, 3291 (1994); J.G. Körner, E. Mirkes, G.A. Schuler, *Int. J. Mod. Phys.* **A4**, 1781 (1989); T. Brodkorb, J.G. Körner, *Z. Phys.* **C54**, 519 (1992).
[11] D. Graudenz, PROJET3.6 manual, unpublished.
[12] I. Abt, *et al.*, (H1 Collaboration), *Z. Phys.* **C61**, 59 (1994).
[13] G. Ingelman, LEPTO6.1, Proc. Workshop Physics at HERA, DESY, Hamburg, Vol. 3, 1991, p 1366.
[14] R. Nisius, PhD thesis, Aachen preprint, PITHA 94/21 (1994).
[15] Particle Data Group, *Phys. Rev.* **D45**, (1992).
[16] Yu.L. Dokshitzer, *et al., Basics of Perturbative QCD,* Editions Frontiers, Paris 1991; Yu.L. Dokshitzer, V.A. Khoze, S.I.Troyan, *Z. Phys.* **C55**, 107 (1992).
[17] OPAL Collaboration, *Phys. Lett.* **247B**, 617 (1990).
[18] Studies of Charged Particles in the Breit Frame, Contribution of the ZEUS Collaboration at the 27th International Conference on High Energy Physics, Glasgow, UK, July 1994.
[19] Studies of Charged Particles in the Breit Frame, Contribution of the H1 Collaboration at the 27th International Conference on High Energy Physics, Glasgow, UK, July 1994.

[20] M. Derrick, *et al.*, (ZEUS Collaboration), *Phys. Lett.* **B315**, 481 (1993).
[21] T. Ahmed, *et al.*, (H1 Collaboration), DESY preprint DESY 94-133, 1994.
[22] M. Derrick, *et al.*, (ZEUS Collaboration), DESY preprint DESY 94-063, 1994.
[23] H. Jung, DESY preprint DESY 93-182, 1993.
[24] P. Bruni, G. Ingelman, DESY preprint DESY 93-187, 1993; Proc. Europhysics Conf. on HEP, Marseille 1993.
[25] N.N. Nikolaev, B.G. Zakharov, *Z. Phys.* **C53**, 331 (1992).